Biochimica et Biophysica Acta 1840 (2014) 3042–3051

Contents lists available at ScienceDirect

Biochimica et Biophysica Acta

journal homepage: www.elsevier.com/locate/bbagen

Pre-steady-state fluorescence analysis of damaged DNA transfer from human DNA glycosylases to AP endonuclease APE1

Alexandra A. Kuznetsova [a,1], Nikita A. Kuznetsov [a,b,*,1], Alexander A. Ishchenko [c], Murat K. Saparbaev [c], Olga S. Fedorova [a,b,**]

[a] Institute of Chemical Biology and Fundamental Medicine, Novosibirsk 630090, Russia
[b] Department of Natural Sciences, Novosibirsk State University, Novosibirsk 630090, Russia
[c] Groupe «Réparation de l'ADN», Université Paris-Sud XI, UMR8200 CNRS, Institut Gustave Roussy, Villejuif Cedex F-94805, France

ARTICLE INFO

Article history:
Received 8 May 2014
Received in revised form 8 July 2014
Accepted 22 July 2014
Available online 31 July 2014

Keywords:
Base excision repair
DNA glycosylase
AP endonuclease
Protein–protein interaction
Coordination of DNA repair process

ABSTRACT

Background: DNA glycosylases remove the modified, damaged or mismatched bases from the DNA by hydrolyzing the N-glycosidic bonds. Some enzymes can further catalyze the incision of a resulting abasic (apurinic/apyrimidinic, AP) site through β- or β,δ-elimination mechanisms. In most cases, the incision reaction of the AP-site is catalyzed by special enzymes called AP-endonucleases.
Methods: Here, we report the kinetic analysis of the mechanisms of modified DNA transfer from some DNA glycosylases to the AP endonuclease, APE1. The modified DNA contained the tetrahydrofurane residue (F), the analogue of the AP-site. DNA glycosylases AAG, OGG1, NEIL1, MBD4^{cat} and UNG from different structural superfamilies were used.
Results: We found that all DNA glycosylases may utilise direct protein–protein interactions in the transient ternary complex for the transfer of the AP-containing DNA strand to APE1.
Conclusions: We hypothesize a fast "flip-flop" exchange mechanism of damaged and undamaged DNA strands within this complex for monofunctional DNA glycosylases like MBD4^{cat}, AAG and UNG. Bifunctional DNA glycosylase NEIL1 creates tightly specific complex with DNA containing F-site thereby efficiently competing with APE1. Whereas APE1 fast displaces other bifunctional DNA glycosylase OGG1 on F-site thereby induces its shifts to undamaged DNA regions.
General significance: Kinetic analysis of the transfer of DNA between human DNA glycosylases and APE1 allows us to elucidate the critical step in the base excision repair pathway.

© 2014 Elsevier B.V. All rights reserved.

1. Introduction

Exposure of cellular DNA to reactive oxygen species (ROS), generated either by normal cell metabolism or by chemical and physical exogenous agents, leads to various lesions. A DNA lesion may be mutagenic and block replication and transcription [1]. Failure to repair DNA can lead to mutations, genomic instability, premature ageing, mental retardation, or other developmental disorders and cancer [2–8]. Over several decades, DNA damage and repair mechanisms have been the focus of numerous investigations, including structural, biochemical, and genetic studies on organisms ranging from bacteria to humans [9–15].

One of the major pathways to remove DNA lesions is the base excision repair (BER). BER pathway is a multi-step process, and can be reconstituted with a limited number of proteins. It involves a cascade of enzymes, which typically begins with a damage-specific DNA glycosylases that interact with DNA to specifically find target damaged bases ([16] and references therein) and cleave the N-glycosidic bond of the lesion. This generates an abasic (apurinic/apyrimidinic (AP)) site [17]. The toxic AP-intermediates must be recognized and processed by AP endonuclease immediately after the action of a DNA glycosylase [18–21]. Bifunctional DNA glycosylases can also catalyze a β- or β,δ-elimination reaction (AP-lyase activity) to affect the strand scission after base removal. Short patch BER requires two additional enzymes to replace the damaged nucleotide: DNA polymerase β and DNA ligase III/XRCC1 heterodimer or DNA ligase I [22–25].

Coordination of the enzymatic activities of DNA glycosylases and AP endonuclease is essential to ensure a complete repair of the damaged bases. One of the major questions remains unanswered: how the exchange of damaged DNA occurs. It was previously suggested that the

Abbreviations: aPu, 2-aminopurine; AP, apurinic/apyrimidinic site; BER, base excision repair; ODN, oligodeoxyribonucleotide; F, (3-hydroxytetrahydrofuran-2-yl)methyl phosphate

* Correspondence to: N.A. Kuznetsov, Institute of Chemical Biology and Fundamental Medicine, Novosibirsk 630090, Russia. Tel.: +7 383 3635175; fax: +7 383 3635153.
** Correspondence to: O.S. Fedorova, Institute of Chemical Biology and Fundamental Medicine, Novosibirsk 630090, Russia. Tel.: +7 383 3635174; fax: +7 383 3635153.
E-mail addresses: nikita.kuznetsov@niboch.nsc.ru (N.A. Kuznetsov), fedorova@niboch.nsc.ru (O.S. Fedorova).
[1] A.A.K. and N.A.K. contributed equally to this work.

http://dx.doi.org/10.1016/j.bbagen.2014.07.016
0304-4165/© 2014 Elsevier B.V. All rights reserved.

enzymatic steps in BER may involve recognition of a product–enzyme complex by the next enzyme in the pathway, rather than binding to an intermediate that is free in solution [26–29]. A "passing-the-baton" model proposed for BER is consistent with the findings that DNA glycosylases coordinate with other proteins to process the damaged DNA substrate. The resulting DNA product is efficiently passed to the next enzyme, just as a baton is passed from one runner to the next.

Previous studies of the protein–protein interactions between BER enzymes showed that AP endonuclease enhances the turnover of many DNA glycosylases. For instance, AP-endonuclease APE1 enhances uracil DNA glycosylase hUNG activity, acting much like a "snow plow" in the DNA minor groove, thereby inducing hUNG release [30]. The AP-sites generated by another DNA glycosylase, human 8-oxoguanine DNA glycosylase OGG1, can be occupied by APE1, avoiding the re-association with OGG1 [31,32]. This process shifts the equilibrium towards the free OGG1, making it available to initiate new catalytic cycles. A recent study on OGG1 suggests that APE1 specifically recognizes an OGG1/DNA complex, distorts a stretch of DNA 5′ to the OGG1 molecule, and actively displaces this glycosylase from the lesion [33]. Moreover, stimulation of human MutY homolog (MYH) by APE1 appears to involve protein–protein interactions [34–36]. In fact, studies in *Escherichia coli* showed the influence of the AP endonucleases, Exo III and Endo IV, on MutY activity, providing evidence for an interaction between the MutY-product DNA complex and Exo III or Endo IV [37]. APE1 also significantly increases the rate of dissociation of thymine DNA glycosylase TDG from AP-sites, presumably through direct interaction with the bound DNA glycosylase [38–41]. It was suggested that the initial contact site for APE1 is the "insertion loop" of TDG, which plays a key role in substrate recognition and nucleotide flipping, and may also disrupt the DNA phosphate contacts [42]. These interactions could conceivably promote dissociation of the product complex. Recently, it was demonstrated that nonspecific DNA binding coordinated both APE1 and alkyladenine DNA glycosylase AAG, thereby stimulating AAG turnover [43,44]. It was shown [43,45] that full-length AAG and an N-terminal deletion mutant missing the first 79 amino acids have similar base excision activity and APE1 stimulates the multiple-turnover both forms of AAG.

Although the detailed molecular mechanism of DNA glycosylase stimulation by APE1 remains unknown, and additional studies are needed to fully elucidate the mechanism by which APE1 disrupts the DNA glycosylase-product complex, we postulate the following basic ideas. The first idea suggests that APE1 stimulates DNA glycosylase turnover by simply depleting the concentration of unbound AP-DNA. The DNA product containing 5′-nicked AP-site has less inhibitory effect on DNA glycosylases. The second mechanism requires a direct interaction between APE1 and the DNA glycosylase/AP-DNA complex, and induces DNA glycosylase release to facilitate the process of AP-DNA cleavage by APE1.

For each type of damage, there is typically one enzyme, or a small group of enzymes, which removes the damaged base to produce an abasic site. Human DNA glycosylases belong to different structural families, and do not have common interaction surfaces. This raises the obvious question of how different DNA glycosylases interact with the same enzyme, APE1, to coordinate the initial stages of BER.

In this study, we focused on the issue of DNA transfer from human DNA glycosylases [AAG, OGG1, NEIL1, MBD4^{cat} (catalytic domain of MBD4) and UNG] to AP-endonuclease APE1. We analyzed this process using oligonucleotide substrates containing tetrahydrofuran AP-site analogue (F-site) placed in different positions of the DNA duplexes. The tetrahydrofuran residue does not contain an OH-group at C1′-atom. It is non-cleavable by both monofunctional DNA glycosylases (AAG, MBD4^{cat} and UNG) and, bifunctional DNA glycosylases (OGG1, NEIL1), but is recognized and processed by APE1. The direct measurement of the pre-steady-state binding and the cleavage of the model DNA duplexes containing the F-site, in the presence of DNA glycosylases and APE1, revealed the most probable mechanism of DNA transfer from one enzyme to another. The data obtained support the idea that the process of DNA transfer includes formation of a transient ternary complex through the rotation of DNA glycosylase and APE1 around DNA double helix. We suggest that a fast "flip-flop" exchange of damaged and undamaged DNA strands occurs in this complex. These results provide insight into the mechanism of coordination between DNA glycosylase and AP endonuclease activities.

2. Material and methods

2.1. Reagents

The chemicals used were purchased mainly from Sigma-Aldrich. T4 polynucleotide kinase was purchased from New England Biolabs (Beverly, MA). γ[32P]-ATP (~3000 Ci/mmol) was purchased from Radioisotope (Moscow). Unless indicated otherwise, all experiments were carried out at 25 °C in a reaction buffer containing 50 mM Tris–HCl (pH 7.5), 50 mM KCl, 1 mM EDTA, 1 mM dithiothreitol, 5 mM $MgCl_2$ and 9% glycerol (v/v).

2.2. Oligonucleotides

The oligodeoxyribonucleotides (ODNs) (Table 1) were synthesized from commercially available phosphoramidites (Glen Research, Sterling, VA), using an ASM-700 synthesizer (BIOSSET, Novosibirsk, Russia), and purified by HPLC, as described elsewhere [46].

2.3. Enzymes

AAG with the first 73 amino acids deleted from the N-terminus was used in this study. The AAG protein was purified as described previously [47]. The purification of human 8-oxoguanine DNA glycosylase OGG1 was performed as described [48]. AP endonuclease APE1 and human DNA glycosylase NEIL1 were expressed and purified in their native form without tags or other modifications as described previously [49,50]. The catalytic domain of MBD4^{cat} (residues 426–580) was purified as described [51].

Wild-type full-length nuclear form of human uracil DNA glycosylase UNG was expressed in Rosetta 2(DE3) *E. coli* cells. Briefly, cells containing the UNG encoding vector were grown in 1 l of LB medium at 37 °C. UNG expression was then induced by the addition of IPTG, and the cells were grown at 37 °C during 6 h. The cells were then harvested by centrifugation and then resuspended in buffer (20 mM HEPES–KOH pH 7.6, 20 mM NaCl, 1 mM DTT) followed by cell lysis using a French press. The homogenate was centrifuged at 40,000 ×*g* for 40 min and the

Table 1
DNA substrates used in this study.

F12	5′-d(CTCTC **F aPu** CTTCC)-3′
	3′-d(GAGAGG C GAAGG)-5′
F30-3′	5′-d(GTCACCACTGCTCATGTGCATA **F aPu** CATGTG)-3′
	3′-d(CAGTGGTGACGAGTACACGTATG C GTACAC)-5′
F30-5′	5′-d(GTGCATA **F aPu** CATGTGTGTCACCACTGCTCA)-3′
	3′-d(CACGTATG C GTACACACAGTGGTGACGAGT)-5′

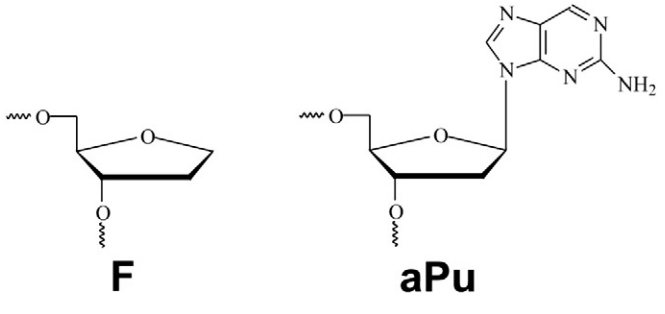

supernatant was passed through a column packed with 50 ml of Q-Sepharose Fast Flow resin (Amersham Biosciences, Uppsala, Sweden) pre-equilibrated in the same buffer. All purification procedures were carried out at 4 °C. The flow-through fractions containing UNG were pooled and loaded onto a 1 ml HiTrap-Heparin™ column (Amersham Biosciences, Uppsala, Sweden). Bound proteins were eluted in a 50–600 mM NaCl gradient. The purified protein was then dialyzed and concentrated into 10 mM sodium phosphate pH 8.0, 150 mM NaCl, 1 mM DTT and 50% glycerol and then stored at −20 °C. The concentrations of UNG stock solutions were determined using the absorbance at 280 nm and an extinction coefficient of 50,608 M^{-1} cm^{-1}.

The activity of the various proteins was tested by using their classical substrates and was checked just before their use.

2.4. Stopped-flow fluorescence measurements

The pre-steady state kinetics was studied using stopped-flow technique with fluorescence detection as previously described [52–54], using an SX20 stopped-flow spectrometer (Applied Photophysics). To detect 2-aminopurine fluorescence, $\lambda_{ex} = 310$ nm was used, and the emission was followed at $\lambda_{em} \geq 370$ nm (Corion filter LG-370). The dead time of the instrument was 1.4 ms. Concentrations of APE1 and F-substrates were 1 μM, and concentrations of DNA glycosylases were 2 μM, in all experiments. Concentrations of reactants reported are those in the reaction chamber after mixing. Typically, each trace shown is an average of three or more individual experiments. The experimental errors were less than 5%.

Data obtained from the fluorescence stopped-flow kinetic assays were fitted by the following exponential Eq. (1), using Origin software (Originlab Corp.):

$$F = F_0 + F_1 \exp\left(-k_1^{aPu} t\right) + F_2 \exp\left(-k_2^{aPu} t\right) \quad (1)$$

where F is the observed aPu fluorescence intensity, F_0 is the background fluorescence, F_i is the fluorescence parameter and k_i^{aPu} is the observed rate constant.

2.5. PAGE time-course experiments

Single-turnover APE1 endonuclease assays were performed in the standard reaction buffer. The reaction solution contained 1.0 μM APE1, 1.0 μM ODN substrate and 2.0 μM DNA glycosylases. The F-substrates were initially incubated with specific DNA glycosylase (5 min) to form the complex. The cleavage of the F-substrate was initiated by the addition of APE1. 2 μl aliquots of the reaction mixture were withdrawn at time intervals of 7, 12, 17, 22, 30, 60 and 120 s, immediately quenched with 3 μl of gel-loading dye containing 7 M urea and 50 mM EDTA, and loaded on a 20% (w/v) polyacrylamide/7 M urea gel. The disappearance of the substrate and product formation were analyzed by autoradiography, and quantified by scanning densitometry using Gel-Pro Analyzer v4.0 software (Media Cybernetics, Bethesda, MD).

The fraction product was fitted by the single exponential curve using Origin software (Originlab Corp.) (Eq. (2)).

$$[\text{product}] = A \times \left[1 - \exp\left(-k^{PAAG} t\right)\right] \quad (2)$$

where A is the amplitude, k^{PAAG} is the rate constant, and t is the reaction time (s).

Multiple-turnover APE1 endonuclease assays were performed in the same way like single-turnover experiments. Typically, the APE1 concentration of substrate was 0.1 μM, the concentration of substrate was 1.0 μM and the concentration of DNA glycosylase was 2.0 μM. 2 μl aliquots of the reaction mixture were withdrawn at 7, 12, 20, 30, 60, 120, 180, 240, 360, 600, 900 and 1200 s, immediately quenched with 3 μl of gel-loading dye containing 7 M urea and 50 mM EDTA, and loaded on a 20% (w/v) polyacrylamide/7 M urea gel.

3. Results and discussion

3.1. Rationale

To study the mechanism of F-site transfer between DNA glycosylases and APE1, three types of model DNA duplexes were designed (Table 1). The model DNA duplexes contained a single tetrahydrofuran residue F. The size of the recognition site for all examined DNA glycosylases and APE1 does not exceed 12 bp [55]. Therefore, short 12 bp and 30 bp DNA duplexes were used as substrates for DNA glycosylases. The 12 bp duplex, F12, contained the F-residue in the central part, and provided the binding site for one enzyme only. The 30 bp DNA duplexes, F30-5′ and F30-3′, each contained the F-residue located 8 bp away from 5′- or 3′-terminus, respectively, and provided the opportunity for simultaneous binding of DNA glycosylase and APE1.

Conformational changes in DNA were recorded using 2-aminopurine (aPu) as a fluorescent marker. 2-Aminopurine label was placed on the 3′-side of the F-site. The aPu fluorescence has high sensitivity to the microenvironment, and allows monitoring processes, which lead to conformation changes in the DNA [52,53,56–58].

To determine the possible mechanism of APE1 displacing the DNA glycosylases bound to DNA containing the F-site, the stopped-flow kinetic experiments under single-turnover conditions were performed. Fig. 1 schematically demonstrates the experimental strategy used for detecting the aPu fluorescence in F-containing DNA-substrate. First, the interaction of F-substrates with DNA glycosylases was studied (Fig. 1A). Here, any changes induced in aPu fluorescence would be a read-out for binding of the DNA glycosylase to the F-substrate to form a specific complex. Second, the binding and cleavage of the F-substrates by APE1 were studied (Fig. 1B). Finally, the F-substrates were pre-incubated with the DNA glycosylases to form the complex enzyme–substrate, and then mixed with APE1 (Fig. 1C). Using short and long asymmetric DNA-substrates, the role of direct protein–protein interactions, and the effect of 5′- or 3′-flanking undamaged DNA regions in the process of F-site transfer, between DNA glycosylases and APE1 was elucidated.

3.2. Interaction of DNA glycosylases with DNA containing F-site

3.2.1. OGG1

The binding of human DNA glycosylase OGG1 to the short (12 bp) and the long (30 bp) F-substrates was essentially completed in 1 s, based on the maxima locations of the aPu fluorescence traces (Fig. 2A–C). Interestingly, the characteristic phases of the increase and the decrease of aPu fluorescence occurred in the different time ranges for the short and long duplexes, indicating the participation of nonspecific binding while searching for the F-site.

The 12 bp substrate is near to minimal size bound by DNA glycosylases. Therefore, in the cases of long 30 bp DNA substrates (at molar ratio DNA:enzyme = 1:1) 2.5 times excess of binding sites is present. It means that the effect of increased concentration of DNA should be observed in the cases of long substrates for all DNA glycosylases. For hOGG1 this effect is more expressed due to higher total fluorescence changes. Additionally, the long substrates give possibility to enzyme for random non-specific DNA binding with subsequent enzyme sliding to search the F-site. 1D-sliding of OGG1 along DNA has very high rate [59]. Both of these factors lead to observed acceleration of initial increase phase.

Increase in the aPu fluorescence intensity reflects a transition of the 2-aminopurine to a more hydrophilic environment, indicating partial “melting” of the duplex in the primary enzyme–DNA complex [52,60,61]. This increase is followed by a decrease in aPu fluorescence intensity, independent of the used substrate. The decrease reflects the bending of

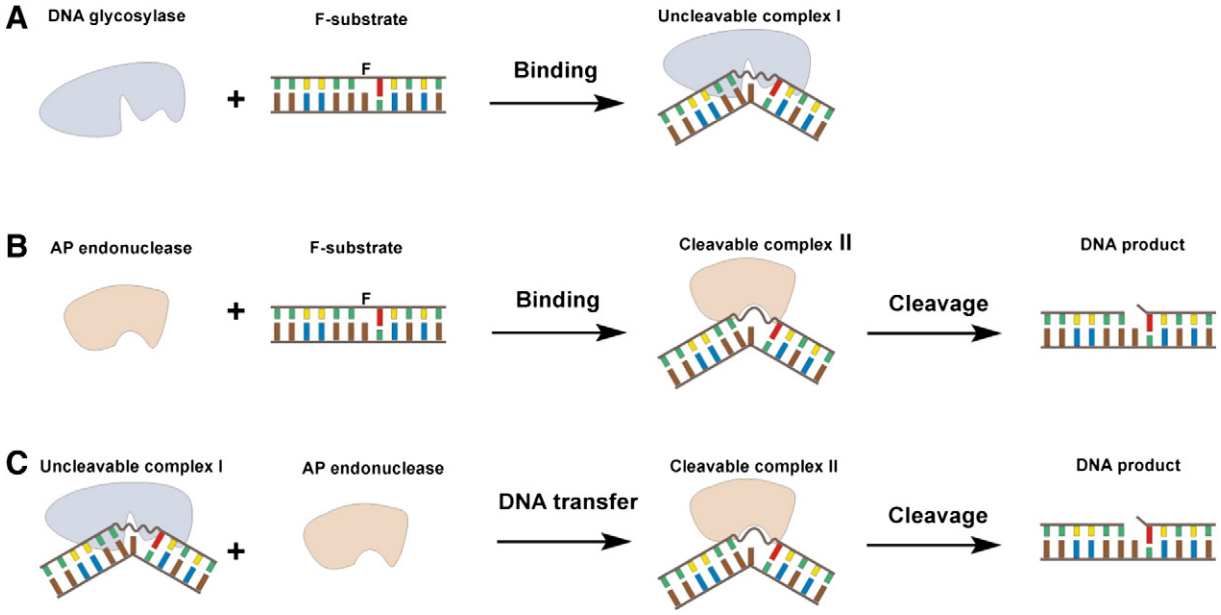

Fig. 1. Schematic representation of the mechanisms of (A) the interaction of DNA glycosylases with F-substrate, resulting in the formation of the uncleavable complex I; (B) the interaction of APE1 with F-substrate, resulting in the formation of the catalytically active complex II, and subsequent cleavage of DNA; (C) the interaction of APE1 with DNA glycosylase/F-substrate uncleavable complex I with subsequent DNA transfer, formation of cleavable complex II, and cleavage of the F-substrate by APE1.

the DNA chain at the AP-site region, and the transition of the aPu residue to a more hydrophobic environment of the OGG1 active site. It potentially leads to filling the abasic void in the DNA duplex by Tyr-203, Arg-154, Arg-204 and Asn-149 amino acid residues of OGG1 [52,60,62].

3.2.2. MBD4^{cat}

Stopped-flow kinetic curves characterizing the MBD4^{cat} interaction with F-substrates were similar to the results observed for OGG1 (Fig. 2A–C). In all cases, the resulting curves demonstrated two types of changes in the fluorescence signal: an increase followed by a decrease. The maxima values on these curves were located at 0.2 s, 0.08 s and 0.06 s for F12, F30-5′ and F30-3′ substrates, respectively. Despite different substrate specificities, MBD4^{cat} belongs to the same structural superfamily of DNA glycosylases HhH (helix–hairpin–helix) as OGG1. Therefore, it is reasonable to propose that the interaction of MBD4^{cat} with F-substrates results in similar DNA conformational changes as detected for OGG1, including the primary melting and bending of the DNA chain, followed by filling the abasic void with MBD4^{cat} amino acids.

3.2.3. NEIL1

The processes of NEIL1 binding to the F-substrates were essentially completed within 10 s (Fig. 2). The one-phase change in the aPu fluorescence intensity was observed that could be the result of filling the abasic void in the DNA duplex with the enzymes' amino acids. It is known that NEIL1 utilises the amino acid residues Met-80, Arg-117 and Phe-119 [63].

3.2.4. AAG

The processes of AAG binding to DNA depend on the used F-substrates. In the case of AAG interacting with F30-5′ substrate the tiny increase, probably due to DNA "melting" upon enzyme binding, was detected up to 6 ms followed by a decrease of aPu fluorescence. The slight decrease of aPu fluorescence can be explained the fact that only Tyr-162 is inserted into the abasic void [64,65]. For F12 substrate the single decrease phase was detected and for F30-3′ substrate no changes were observed. The difference of fluorescence curves for used model F-substrates indicates the different importance of 5′- and 3′-adjacent non-specific regions of DNA in the process of F-site recognition.

3.2.5. UNG

The stopped-flow kinetic curves obtained by UNG interaction with all F-substrates did not display the noticeable aPu fluorescence change seen for other enzymes (Fig. 2A–C). Of note, UNG utilises the single amino acid Leu-272 to insert into DNA. Moreover, UNG creates a DNA kink, ~45° at the abasic site [30], whereas for OGG1 and MBD4^{cat} this angle is equal to ~70° [66] and ~57° [67], respectively. Therefore, it is likely that such a low alteration in the DNA conformation does not result in a significant change of hydrophobicity in the vicinity of aPu residue.

To summarise, the DNA glycosylases used in this study possess different architectures, and belong to four structural superfamilies. OGG1 and MBD4^{cat} belong to the helix–hairpin–helix (HhH) superfamily; NEIL1 and AAG belong to the H2TH (helix-two turn-helix or Fpg/Nei) and alkyladenine DNA-glycosylase superfamilies, respectively. UNG is the member of the UDG superfamily. It is interesting to note that both enzymes of HhH superfamily, OGG1 and MBD4^{cat}, caused pronounced changes in aPu fluorescence, indicating the formation of similar contacts in the complex with F-containing DNA. Moreover, these changes were independent of the difference in substrate specificity and the type of catalysis (monofunctional MBD4^{cat} or bifunctional OGG1). NEIL1 and AAG also demonstrated the two-phase change of aPu fluorescence signals, which were more prominent for short 12 bp DNA substrate, F12. The member of the UDG superfamily, UNG, induced only minor changes in the aPu fluorescence signal. This minor change indicates a "minor" conformational alteration of the abasic DNA during the complex formation, and probably, a concerted rearrangement of the DNA-structure, which does not change the polar properties of aPu's surrounding environment.

3.3. Interaction of AP endonuclease APE1 with DNA containing F-site

The aPu fluorescence curves obtained for the interaction of APE1 with F-substrates were characterized with two phases: an initial decrease of fluorescence intensity followed by its increase (Fig. 3). It should be noted that for long substrates, F30-3′ and F30-5′, the first phase was less pronounced (Fig. 3B and C) in comparison to the short F12 substrate (Fig. 3A). It was previously shown [58] that DNA cleavage catalyzed by APE1, is accompanied by concerted structural rearrangements within the enzyme and the DNA molecules inside of the

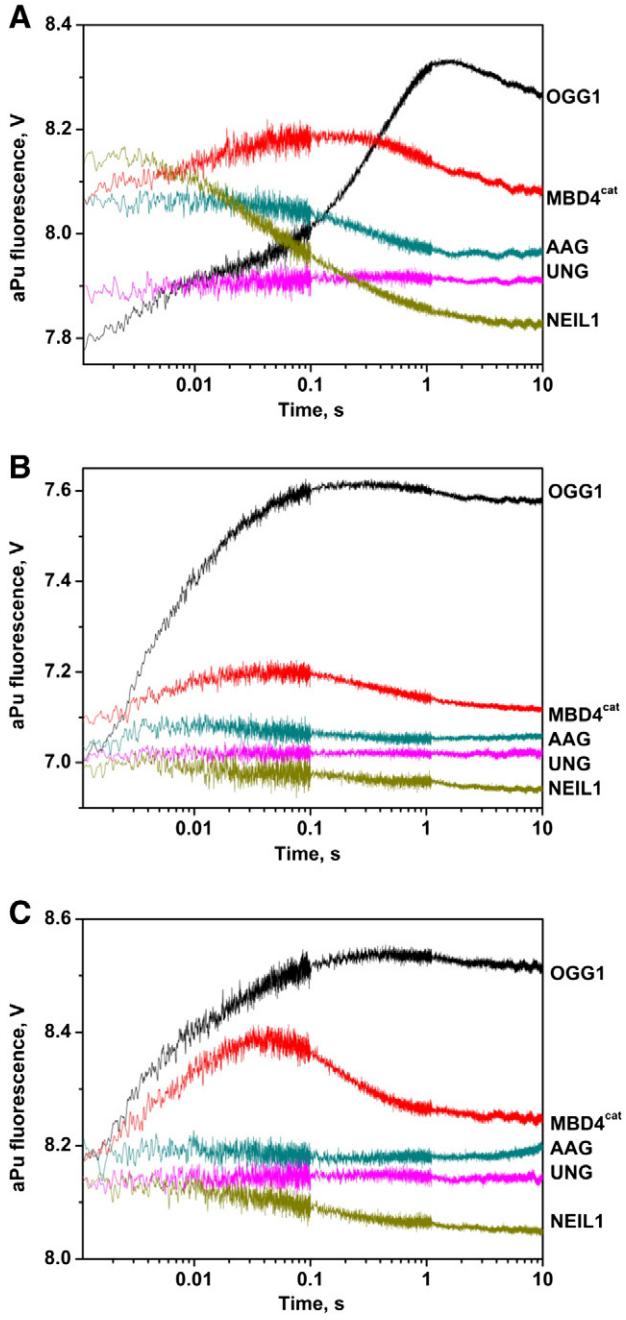

Fig. 2. The stopped-flow fluorescent traces obtained for the binding of F12- (A), F30-5′- (B) and F30-3′-substrates (C) by DNA glycosylases. Concentrations of OGG1, MBD4^{cat}, NEIL1, AAG and UNG were 2.0 μM, DNA concentration was 1.0 μM.

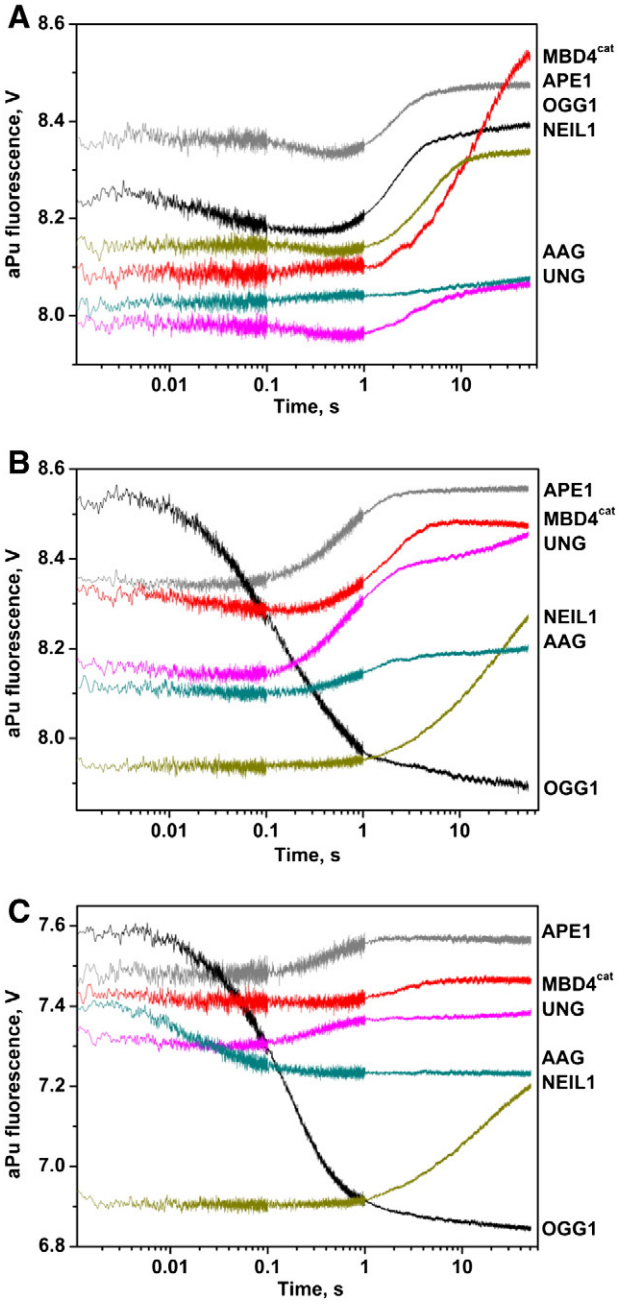

Fig. 3. The stopped-flow fluorescent traces obtained for substrate binding and cleavage of (A) F12, (B) F30-5′ and (C) F30-3′ by APE1 alone, and in the presence of different DNA glycosylases. Concentration of APE1 was 1.0 μM, concentrations of OGG1, MBD4^{cat}, NEIL1, AAG and UNG were 2.0 μM, DNA concentration was 1.0 μM.

enzyme–substrate complex. The fluorescence kinetic curves were analyzed using the exponential Eq. (1) (see Experimental Procedures). The first phase, characterized by the rate constant k_1^{aPu} (see Table 2), most likely corresponds to the initial binding, and adjustment of the DNA structure for catalysis. The second phase characterized by the rate constant k_2^{aPu} should correspond to the DNA cleavage step and release of the DNA product from the complex with APE1.

In addition to stopped-flow fluorescence data, a denaturing PAGE analysis of the accumulation of the reaction products with ^{32}P-labelled F-substrates in single (Fig. 4) and multiple (Fig. 5) turnovers was performed. This allowed a direct association between the DNA conformational transitions, represented by aPu fluorescence intensity changes, and the exact chemical reaction steps. The time courses of product accumulation demonstrated a rapid formation of the incised products. The results of the chemical quench assay evidently confirmed that the sharp increase in aPu fluorescence, observed in the stopped-flow traces, corresponds to the DNA cleavage step and release of the DNA product from the complex with APE1.

3.4. Interaction of AP endonuclease APE1 with complexes of DNA glycosylases and DNA containing F-site

To study the interaction of APE1 with the DNA glycosylase–DNA containing F-site complex, different DNA glycosylases were each incubated with F-substrates for the formation of enzyme–substrate complexes, which were then mixed with APE1 (see Experimental Procedures).

Table 2
The rate constants for F-substrates' cleavage by APE1, in the presence of different DNA glycosylases, obtained using the fluorescence assay.

Substrates	F12		F30-3′		F30-5′	
Enzymes	k_1^{aPu}, s^{-1}	k_2^{aPu}, s^{-1}	k_1^{aPu}, s^{-1}	k_2^{aPu}, s^{-1}	k_1^{aPu}, s^{-1}	k_2^{aPu}, s^{-1}
APE1 + F	2.2 ± 0.04	0.58 ± 0.01	36 ± 1	1.4 ± 0.01	14 ± 1.8	2.2 ± 0.05
APE1 + (F·OGG1)	10.0 ± 0.1	0.4 ± 0.001	3.7 ± 0.1	–	4.4 ± 0.1	–
APE1 + (F·MBD4^{cat})	–	0.06 ± 0.001	15 ± 0.2	0.54 ± 0.04	8.8 ± 0.3	0.46 ± 0.01
APE1 + (F·NEIL1)	1.2 ± 0.02	0.26 ± 0.001	–	0.05 ± 0.001	–	0.07 ± 0.001
APE1 + (F·AAG)	–	0.13 ± 0.001	32 ± 1.2	0.82 ± 0.01	28 ± 1	–
APE1 + (F·UNG)	3.9 ± 0.1	0.21 ± 0.001	40 ± 1.6	1.1 ± 0.01	20 ± 2	2.7 ± 0.02

The rate constant k_1^{aPu} characterizes the processes of DNA binding and replacement of DNA glycosylases by APE1.
The rate constant k_2^{aPu} characterizes the process of dissociation of APE1 and/or DNA glycosylases from the DNA product.

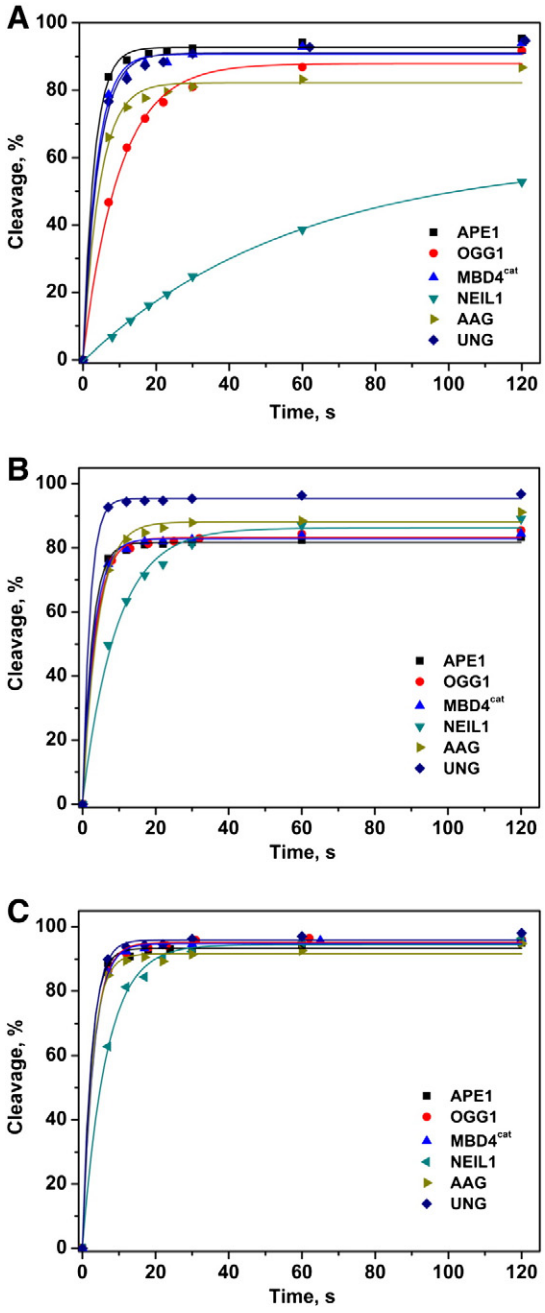

Fig. 4. Cleavage of ^{32}P-labelled F-containing substrates by APE1: alone (■), and in the presence of OGG1 (●), MBD4^{cat} (▲), NEIL1 (▼), AAG (►), and UNG (♦). Time courses of accumulation of the cleaved product for F12- (A), F30-5′- (B) and F30-3′-substrates (C). Concentration of APE1 was 1.0 μM, concentrations of OGG1, MBD4^{cat}, NEIL1, AAG and UNG were 2.0 μM, DNA concentration was 1.0 μM.

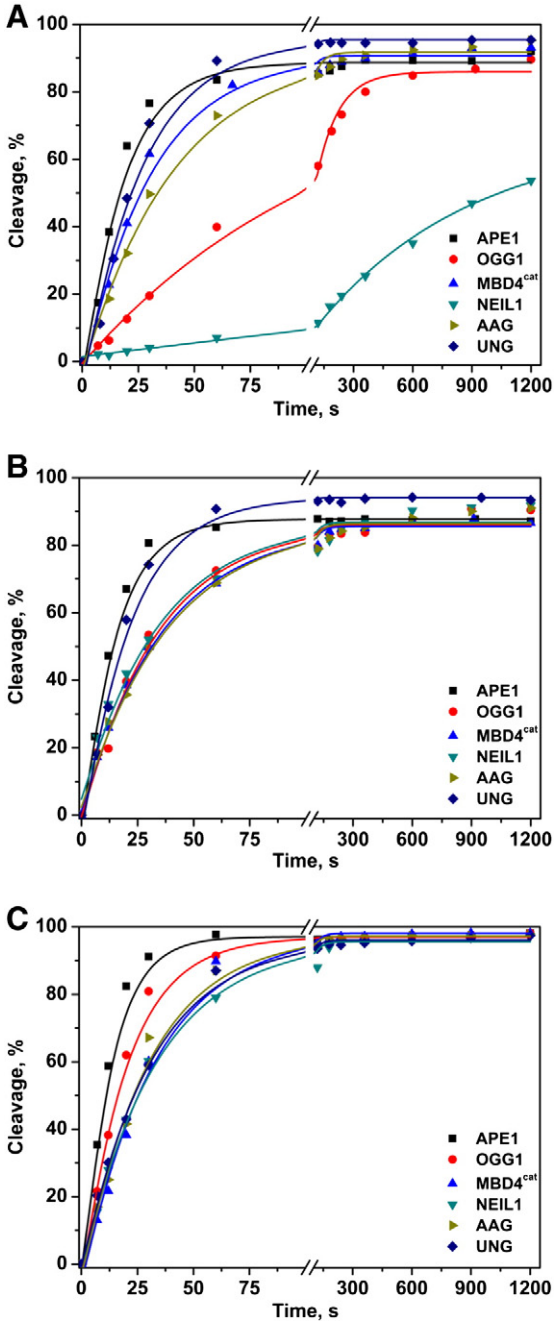

Fig. 5. Cleavage of ^{32}P-labelled F-substrates by APE1 at low concentration: alone (■), and in the presence of OGG1 (●), MBD4^{cat} (▲), NEIL1 (▼), AAG (►) and UNG (♦). Time courses of accumulation of the cleaved product for F12- (A), F30-5′- (B) and F30-3′-substrates (C). Concentration of APE1 was 0.1 μM, concentrations of OGG1, MBD4^{cat}, NEIL1, AAG and UNG were 2.0 μM, DNA concentration was 1.0 μM.

3.4.1. OGG1

Following APE1 incubation with OGG1·F-substrate complexes, significant changes in the aPu fluorescence intensity were observed, corresponding to the transfer of the F-DNA to APE1, and its incision (Fig. 3A–C). The aPu fluorescence curve of the APE1 interaction with the complex OGG1·F12 is characterized with a profile similar to that of the free F12 substrate. The analysis of fluorescence traces, using Eq. (1), resulted in rate constants of the first step k_1^{aPu} that were about five times larger for APE1 interaction with OGG1·F12 complex compared to APE1 interaction with free F12 (see Table 2). This indicates that OGG1 facilitates APE1 binding to DNA. This can be partially explained by the fact that the free 12 bp DNA duplex cannot accommodate both enzymes simultaneously. This leads to the hypothesis that perhaps a transient ternary complex APE1·OGG1·F12 is formed in which OGG1 firstly dissociates from F-site and then APE1 forms complex with unbound F-site. It was found that the rate constant k_2^{aPu} characterizing the release of the DNA product does not depend strongly on the presence of OGG1.

The stopped-flow kinetic curves obtained from the interaction of APE1 with OGG1·F30-3′ and OGG1·F30-5′ complexes were characterized with a single decrease of the fluorescent signal. There are two factors affected on fluorescence intensity. The first, the absence of an increasing phase (characterized by k_2^{aPu}) can be explained by the high affinity of both enzymes APE1 and OGG1 for the long DNA duplex reaction product containing a nick in one of the duplex chains. Indeed, the cleavage of the F12-substrate leads to the formation of short ODNs (n = 5 and 6), which cannot form a stable duplex in the aqueous solution at 25 °C [48]. In contrast, the cleavage of the 30 bp F-substrates F30-3′ and F30-5′ creates a nick in one of the duplex chains that can simultaneously bind in a nonspecific manner to both APE1 and OGG1. The second factor is that the complex formed between OGG1 and the long F30-3′- and F30-5′-substrates (Fig. 2B and C) resulted in a significant initial increase of the aPu fluorescence signal, due to the melting DNA chain. This provided the aPu residues an access to the aqueous polar medium. Therefore, the disruption of this complex by APE1 causes a significant decrease in the fluorescence signal, which hides the growth phase at the APE1 incision of the DNA chain.

The rates of formation of the nicked product were also measured directly by PAGE. For all used DNA substrates, the rapid burst in the product formation kinetic curve was observed in the time range of 10–20 s (Fig. 4). Since the minimal reaction time point on the autoradiograms is technically limited by time of manual operations (7 s), the initial part of the kinetic curve was insufficiently resolved for the correct calculation of the observed rate constant of catalysis according to Eq. (2) (Table 3). Nevertheless, as detected by PAGE (Fig. 4A), the rate of the F12-substrate cleavage by APE1, in the presence of OGG1, was 3.3 times slower than in the absence of OGG1, highlighting the competition between OGG1 and APE1 for the binding site (Table 3). The rate constants of F30-3′- and F30-5′-substrates' cleavage by APE1 do not depend on the presence of OGG1 (Fig. 4B and C).

To overcome the technical limitation of the PAGE analysis, the accumulation of the reaction products was measured under a tenfold deficiency of APE1 over the concentration of the DNA substrate or OGG1·DNA substrate complex (Fig. 5). Under these conditions, APE1 works in the multiple turnover manner that results in the accumulation of a competition effect of up to 6.3 times for the F12-substrate. The F12-substrate cleavage by APE1, in the presence of OGG1, was less effective than the cleavage of F30-3′- and F30-5′-substrates, indicating that undamaged 5′- and 3′-flanking DNA regions are required for APE1 binding, and subsequent OGG1 displacement on the F-site.

It was previously shown that during the simultaneous action of OGG1 and APE1 on a concatemeric DNA, APE1 recognized and bound the distorted OGG1·DNA complex inducing conformational changes in the 5′-adjacent region of DNA [33]. This way, APE1 occupies the AP-site while OGG1 slides away progressively, searching for another damaged base.

Together, the data obtained in this study indicate that APE1 can directly interact with OGG1·DNA complex through an encounter reaction forming the transient ternary complex APE1·OGG1·DNA. For the F12-substrate, it leads to acceleration of the fluorescence decreasing phase, attributed to the specific complex formation. However, for long F30-3′- and F30-5′-substrates, the significant decrease of the fluorescence overlaps the fluorescence signal increase at the substrate cleavage phase. Moreover, these results indicate the absence of a preference for the direction of OGG1 moving away along the DNA helix. If the regions 5′- and 3′-flanking the DNA lesion are not occupied, the shift of OGG1 from the F-site by APE1 may proceed in both directions along the DNA chain. The process of the F-site transfer from OGG1 to APE1 in the ternary complex, leads to the decrease of the observed rate of the DNA cleavage by APE1, detected by PAGE analysis. Interestingly, the F-site transfer proceeds faster for long F30-3′- and F30-5′-substrates than for short F12-substrate, indicating participation of non-occupied, undamaged DNA regions in this process.

3.4.2. MBD4^{cat}

In the case of MBD4^{cat} catalysis, APE1 resulted in a significant delay of the fluorescence increase phase (Fig. 3) in comparison with the reaction without MBD4^{cat}. This delay was larger for F12-substrate than for long F30-3′- and F30-5′-substrates. The accumulation of the reaction products studied by PAGE, in single turnover conditions (Fig. 4), did not show such a delay, due to a delayed time in probe sampling (Table 3). However, under a tenfold deficiency of APE1, a twofold reduction in the rate of the DNA product accumulation was observed (Fig. 5). It could be assumed that APE1 disrupts the MBD4^{cat}·F12 complex by forming a transient ternary complex, in which the F-site is transferred from MBD4^{cat} to APE1. This mechanism is similar to the DNA transfer mechanism proposed for OGG1. Moreover, as both enzymes MBD4^{cat} and APE1 mainly make contact with only one DNA strand [51,67–70], APE1 may bind the DNA strand complementary to the damage containing strand in the ternary complex MBD4^{cat}·F12·APE1. The exchange of two enzymes between the DNA strands may be described by a "flip-flop" mechanism (Fig. 6), representing the simultaneous rotation of DNA glycosylase and APE1 around DNA double helix. In this case, the process of F-site transfer should be independent of the presence of undamaged flanking regions. "Flip-flop" exchange of the damaged and normal complementary strands of DNA between MBD4^{cat} and APE1 leads to the re-location of the F-site to the active site of APE1 and its cleavage. Indeed, our data show that the rate constants (Table 3) of F-site cleavage by APE1, in the presence of MBD4^{cat}, were approximately the same for all types of substrates used. The delay of the aPu fluorescence growth also indicates that the ternary complex APE1·MBD4^{cat}·DNA-product is more stable than the complex APE1·DNA-product. The

Table 3
The rate constant k^{PAAG} (s^{-1}) for F-substrates' cleavage by APE1 in the presence of different DNA glycosylases.

Substrates	F12	F30-3′	F30-5′
Enzymes	Ratio Substrate:Glycosylase:APE1 = 1:2:1		
APE1 + F	0.33 ± 0.03	0.42 ± 0.04	0.38 ± 0.03
APE1 + (F·OGG1)	0.10 ± 0.01	0.33 ± 0.02	0.29 ± 0.03
APE1 + (F·MBD4^{cat})	0.27 ± 0.03	0.33 ± 0.02	0.33 ± 0.02
APE1 + (F·NEIL1)	0.02 ± 0.001	0.15 ± 0.01	0.11 ± 0.01
APE1 + (F·AAG)	0.22 ± 0.02	0.36 ± 0.04	0.24 ± 0.02
APE1 + (F·UNG)	0.24 ± 0.03	0.39 ± 0.04	0.50 ± 0.05
	Ratio Substrate:Glycosylase:APE1 = 1:2:0.1		
APE1 + F	0.057 ± 0.005	0.082 ± 0.005	0.069 ± 0.004
APE1 + (F·OGG1)	0.009 ± 0.0005	0.051 ± 0.003	0.03 ± 0.003
APE1 + (F·MBD4^{cat})	0.033 ± 0.003	0.031 ± 0.003	0.028 ± 0.001
APE1 + (F·NEIL1)	0.002 ± 0.0001	0.030 ± 0.002	0.029 ± 0.003
APE1 + (F·AAG)	0.025 ± 0.002	0.034 ± 0.002	0.026 ± 0.002
APE1 + (F·UNG)	0.038 ± 0.004	0.033 ± 0.001	0.047 ± 0.003

k^{PAAG} (s^{-1}) is calculated using Eq. (2).

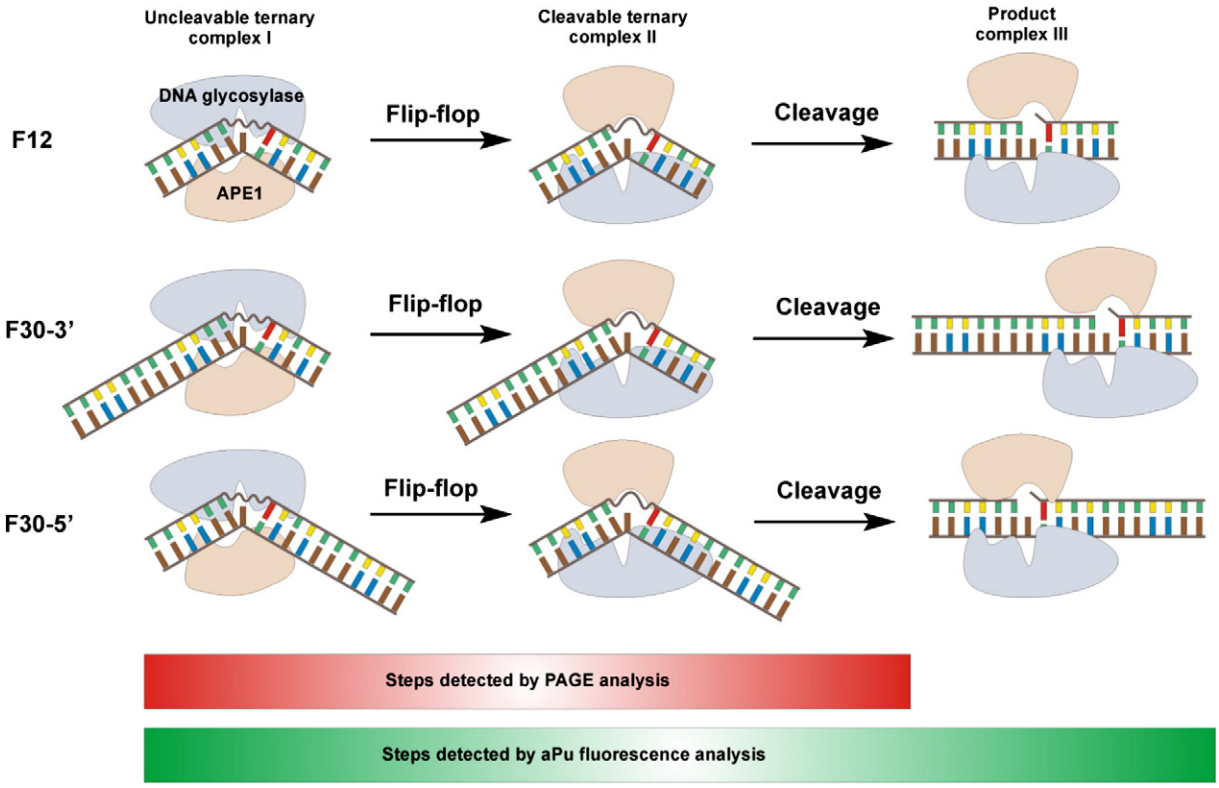

Fig. 6. Schematic representation of the proposed "flip-flop" exchange mechanism. PAGE analysis revealed the steps that comprise exchange of damaged and undamaged DNA strands between DNA glycosylases and APE1, and, the cleavage of the F-site by APE1. The aPu fluorescence analysis additionally illustrates the stability of product complex III, and capacity for non-specific binding of DNA by DNA glycosylases and APE1.

presence of 5′- or 3′-flanking undamaged DNA regions increases the rate constant k_2^{aPu} (Table 2), indicating that these regions may serve as the site where MBD4^{cat} is moved by APE1.

3.4.3. AAG

The observed rate constants, k^{PAAG}, obtained by PAGE analysis of the accumulated reaction products of APE1 action on the free F-containing substrate, or on its complex with AAG, are presented in Table 3. These results indicate a slight decrease in the k^{PAAG} values for reactions between DNA glycosylases and short F12, and long F30-3′ and F30-5′ substrates, in comparison to reactions involving free substrate. This provides evidence for the quick F-site transfer between AAG and APE1 (also see Figs. 4 and 5). At the same time, the shapes of aPu fluorescence traces were significantly different for F12-, F30-3′- and F30-5′-substrates (Fig. 3). For instance, APE1 interaction with AAG·F12 complex (Fig. 3A) demonstrated a weak aPu fluorescence increase, indicating that AAG slightly "melts" the DNA substrate, and remains tightly bound to the DNA product. In contrast, the fluorescence trace of APE1 and AAG·F30-3′ interaction was similar to that of APE1 alone (Fig. 3C). This suggests that the APE1–AAG·F30-3′ complex causes AAG displacement from the F-site, and shifts it to the undamaged 5′-flanking region. Meanwhile, the F-site binding and cleavage in the AAG·F30-5′ complex (Fig. 3B) resulted in a single-step decrease of the aPu fluorescence, as previously observed for OGG1. The shift of AAG, from the F-site to the 3′-flanking undamaged region, leads to the transition of aPu residue to a more hydrophobic environment created by APE1 bound to DNA. Therefore, even after F-site cleavage by APE1, AAG still binds to the 3′-flanking region of the DNA duplex, which contains the aPu residue (Fig. 6).

The significant difference in the aPu fluorescence changes for short and long substrates highlights the importance of nonspecific DNA regions for AAG and APE1 interactions. A recent study [44] proposed that APE1 and AAG are able to bind the DNA duplex simultaneously, as both enzymes predominantly interact with only one of the two DNA strands [64,65]. APE1 stimulates AAG activity by efficiently displacing it from either the 3′- or 5′-side of the abasic site (41). Furthermore, nonspecific DNA interaction was identified as the key mechanism involved in transferring repair intermediates between AAG and APE1 enzymes (41). Importantly, these findings support our hypothesis that AAG is not released into solution, but remains bound to an adjacent undamaged region.

Our data, which shows that AAG and APE1 simultaneously bind one DNA-site, together with previously published results [44], supports the hypothesis that the "flip-flop" exchange of damaged and undamaged strands of DNA may occur in the case of AAG. In reactions involving the long F30-3′- and F30-5′-substrates, AAG can move from the F-site to any undamaged region with approximately the same efficiency. Therefore, the main function of the 5′- and 3′- flanking DNA regions is to provide the space into which AAG is shifted after the F-site is occupied by APE1.

3.4.4. NEIL1

The presence of NEIL1 led to a significant delay of the cleavage of F-substrates by APE1, as revealed by both aPu fluorescence (Fig. 3) and PAGE analysis (Figs. 4 and 5). The data support the suggestion that NEIL1 competes for F-substrates with APE1, resulting in the decrease of the observed rate constants of the F-site cleavage k_2^{aPu} and k^{PAAG}, respectively (Tables 2 and 3). It should be noted that NEIL1 is a bifunctional DNA glycosylase and efficiently catalyzes the cleavage of the native AP-site in β,δ-elimination reaction. NEIL1 creates a tight specific complex with the intermediate product containing the F-site, thereby efficiently competing with APE1.

3.4.5. UNG

Fluorescence kinetic curves, characterizing the interaction of APE1 with UNG·F-DNA complexes, had profiles of a decrease and an increase

in aPu intensity, similar to free F-substrates (Fig. 3). The observed rate constants k_1^{aPu} and k_2^{aPu} (Table 2) were in good agreement with the values obtained for the free substrates, indicating that UNG is easily extruded by APE1, and does not affect the APE1 binding and cleavage of the F-site. Moreover, as revealed by data obtained for the long F30-3′- and F30-5′-substrates, UNG does not stay in the bound state with DNA, and dissociates from the undamaged 5′- or 3′-flanking DNA regions. The PAGE analysis, of the accumulation of reaction products, revealed a slight delay of the F-site cleavage reaction by APE1 under single (Fig. 4) and multiple turnover (Fig. 5) conditions for all used substrates.

Our data clearly demonstrate that APE1 displaces UNG from F-site, independently of the length of the used substrates. Therefore, APE1 extrudes UNG from F-site by direct protein–protein interactions. The existence of such interactions was proposed earlier in structural studies, which revealed that APE1 forms minor groove contacts, and stimulates the turnover of mitochondrial hUNG by extruding it from the AP-site [30,69].

As in the cases of MBD4^{cat} and AAG, the data obtained for UNG can be explained by the formation of the ternary complex, in which, UNG and APE1 bind to damaged and undamaged DNA strands, respectively. The fast "flip-flop" exchange (Fig. 6) of the strands between enzymes leads to the re-location of F-site to the active site of APE1. The similar traits of aPu fluorescence curves, for short and long DNA substrates, indicate that UNG is dissociated from undamaged nonspecific DNA. The fast dissociation of enzyme is in agreement with very short (4 bp) estimated mean of sliding length along DNA for UNG [71], for example the same value for OGG1 is ~400 bp [59].

4. Conclusions

The pre-steady-state kinetic analysis of the interaction between APE1 and the complex DNA glycosylase·F-DNA provides important insights into the mechanism of DNA transfer from DNA glycosylases to APE1. The effect of different DNA glycosylases on the APE1-catalyzed cleavage of the F-containing substrate was studied.

According to our previous kinetic data, the DNA glycosylases [52,60] and APE1 [58] bind damaged and undamaged DNA with near diffusion-limiting rate constants. The association constants of the DNA glycosylases and APE1 with DNA are also nearly equal. In spite of this data, the shapes of the aPu fluorescence kinetic curves reveal the role of the DNA glycosylases in the DNA binding by APE1. These data allow us to propose that the DNA glycosylases OGG1, MBD4^{cat}, AAG and UNG are dislodged by APE1 to non-damaged DNA regions through the "flip-flop" mechanism. The DNA glycosylases OGG1, MBD4^{cat} and AAG stay bound to non-damaged regions and are able to slide away to search for a new lesion in the DNA strand. In contrast, UNG quickly dissociates from damaged DNA after it is cleaved by APE1 as well as from regular nonspecific DNA regions. The bifunctional NEIL1, on the other hand, markedly competes with APE1 for binding DNA containing the F-site, supporting the idea that only NEIL1 recognizes the F-site as its own substrate.

Our findings support the hypothesis that APE1 might be in contact with the DNA strand complementary to the lesion, and both enzymes interact with DNA simultaneously, forming the transient ternary complex. DNA strand exchange, referred in the manuscript as the "flip-flop", represents simultaneous rotation of DNA glycosylases OGG1, MBD4^{cat}, AAG and UNG and APE1 around DNA double helix, which may quickly proceed in this transient complex, providing the F-site cleavage by APE1. The characteristic time of this step is estimated as ~$1/k_1$ (see Fig. 6) and it varies in the range 0.025 s (UNG) to 0.12 s (MBD4^{cat}) according to Table 2 (see data for F30-3′ and F30-5′ substrates). All together, the data obtained in this study support the idea that in spite of the affiliation of DNA glycosylases to the different structural superfamilies, and the absence of similar structural elements for interaction with APE1, these glycosylases may utilise direct protein–protein interactions, in the transient ternary complex, for the exchange of the AP-containing DNA strand between two enzymes in the repair pathway.

Acknowledgements

This work was supported by the Program of the Russian Academy of Sciences "Molecular & Cell Biology" [6.11], the Grants from Russian Foundation for Basic Research [13-04-00013, 14-04-00531 and 14-04-31174], the Grant from Russian Scientific Foundation [14-14-00063] and Ministry of Education and Science [SS-1205.2014.4, SP-4012.2013.4].

References

[1] E.C. Friedberg, G.C. Walker, W. Siede, R.D. Wood, R.A. Schultz, T. Ellenberger, DNA Repair and Mutagenesis, ASM Press, Washington, 2006.
[2] M.F. Denissenko, A. Pao, M. Tang, G.P. Pfeifer, Preferential formation of benzo[a] pyrene adducts at lung cancer mutational hotspots in P53, Science 274 (1996) 430–432.
[3] A.J. van Gool, G.T. van der Horst, E. Citterio, J.H. Hoeijmakers, Cockayne syndrome: defective repair of transcription? EMBO J. 16 (1997) 4155–4162.
[4] A.H. Sarker, S.E. Tsutakawa, S. Kostek, C. Ng, D.S. Shin, M. Peris, E. Campeau, J.A. Tainer, E. Nogales, P.K. Cooper, Recognition of RNA polymerase II and transcription bubbles by XPG, CSB, and TFIIH: insights for transcription-coupled repair and Cockayne Syndrome, Mol. Cell 20 (2005) 187–198.
[5] M. Muftuoglu, J. Oshima, C. von Kobbe, W.H. Cheng, D.F. Leistritz, V.A. Bohr, The clinical characteristics of Werner syndrome: molecular and biochemical diagnosis, Hum. Genet. 124 (2008) 369–377.
[6] S.S. Hecht, Smoking and lung cancer—a new role for an old toxicant? Proc. Natl. Acad. Sci. U. S. A. 103 (2006) 15725–15726.
[7] M.S. Cooke, M.D. Evans, M. Dizdaroglu, J. Lunec, Oxidative DNA damage: mechanisms, mutation, and disease, FASEB J. 17 (2003) 1195–1214.
[8] M.D. Evans, M. Dizdaroglu, M.S. Cooke, Oxidative DNA damage and disease: induction, repair and significance, Mutat. Res. 567 (2004) 1–61.
[9] M.W. Germann, C.N. Johnson, A.M. Spring, Recognition of damaged DNA: structure and dynamic markers, Med. Res. Rev. 32 (2012) 659–683.
[10] M. Lukin, C. de Los Santos, NMR structures of damaged DNA, Chem. Rev. 106 (2006) 607–686.
[11] T.A. Kunkel, D.A. Erie, DNA mismatch repair, Annu. Rev. Biochem. 74 (2005) 681–710.
[12] C.L. Peterson, J. Cote, Cellular machineries for chromosomal DNA repair, Genes Dev. 18 (2004) 602–616.
[13] L. Gros, M.K. Saparbaev, J. Laval, Enzymology of the repair of free radicals-induced DNA damage, Oncogene 21 (2002) 8905–8925.
[14] S.S. David, S.D. Williams, Chemistry of glycosylases and endonucleases involved in base-excision repair, Chem. Rev. 98 (1998) 1221–1261.
[15] A.A. Kuznetsova, D.G. Knorre, O.S. Fedorova, Oxidation of DNA and its components with reactive oxygen species, Russ. Chem. Rev. 78 (2009) 659–678.
[16] A.J. Lee, D.M. Warshaw, S.S. Wallace, Insights into the glycosylase search for damage from single-molecule fluorescence microscopy, DNA Repair (Amst) 20 (2014) 23–31.
[17] C.D. Mol, S.S. Parikh, C.D. Putnam, T.P. Lo, J.A. Tainer, DNA repair mechanisms for the recognition and removal of damaged DNA bases, Annu. Rev. Biophys. Biomol. Struct. 28 (1999) 101–128.
[18] R.P. Cunningham, DNA glycosylases, Mutat. Res. 383 (1997) 189–196.
[19] H. Ide, M. Kotera, Human DNA glycosylases involved in the repair of oxidatively damaged DNA, Biol. Pharm. Bull. 27 (2004) 480–485.
[20] E. Seeberg, L. Eide, M. Bjoras, The base excision repair pathway, Trends Biochem. Sci. 20 (1995) 391–397.
[21] T.K. Hazra, A. Das, S. Das, S. Choudhury, Y.W. Kow, R. Roy, Oxidative DNA damage repair in mammalian cells: a new perspective, DNA Repair (Amst) 6 (2007) 470–480.
[22] Y. Kubota, R.A. Nash, A. Klungland, P. Schar, D.E. Barnes, T. Lindahl, Reconstitution of DNA base excision-repair with purified human proteins: interaction between DNA polymerase β and the XRCC1 protein, EMBO J. 15 (1996) 6662–6670.
[23] D.K. Srivastava, B.J. Berg, R. Prasad, J.T. Molina, W.A. Beard, A.E. Tomkinson, S.H. Wilson, Mammalian abasic site base excision repair. Identification of the reaction sequence and rate-determining steps, J. Biol. Chem. 273 (1998) 21203–21209.
[24] M.L. Hegde, T.K. Hazra, S. Mitra, Early steps in the DNA base excision/single-strand interruption repair pathway in mammalian cells, Cell Res. 18 (2008) 27–47.
[25] A.B. Robertson, A. Klungland, T. Rognes, I. Leiros, DNA repair in mammalian cells: base excision repair: the long and short of it, Cell. Mol. Life Sci. 66 (2009) 981–993.
[26] S.H. Wilson, T.A. Kunkel, Passing the baton in base excision repair, Nat. Struct. Biol. 7 (2000) 176–178.
[27] R. Prasad, D.D. Shock, W.A. Beard, S.H. Wilson, Substrate channeling in mammalian base excision repair pathways: passing the baton, J. Biol. Chem. 285 (2010) 40479–40488.
[28] R. Prasad, W.A. Beard, V.K. Batra, Y. Liu, D.D. Shock, S.H. Wilson, A review of recent experiments on step-to-step "hand-off" of the DNA intermediates in mammalian base excision repair pathways, Mol. Biol. (Mosk) 45 (2011) 586–600.

[29] S.E. Tsutakawa, J. Lafrance-Vanasse, J.A. Tainer, The cutting edges in DNA repair, licensing, and fidelity: DNA and RNA repair nucleases sculpt DNA to measure twice, cut once, DNA Repair (Amst) 19 (2014) 95–107.
[30] S.S. Parikh, C.D. Mol, G. Slupphaug, S. Bharati, H.E. Krokan, J.A. Tainer, Base excision repair initiation revealed by crystal structures and binding kinetics of human uracil-DNA glycosylase with DNA, EMBO J. 17 (1998) 5214–5226.
[31] J.W. Hill, T.K. Hazra, T. Izumi, S. Mitra, Stimulation of human 8-oxoguanine-DNA glycosylase by AP-endonuclease: potential coordination of the initial steps in base excision repair, Nucleic Acids Res. 29 (2001) 430–438.
[32] A.E. Vidal, I.D. Hickson, S. Boiteux, J.P. Radicella, Mechanism of stimulation of the DNA glycosylase activity of hOgg1 by the major human AP endonuclease: bypass of the AP lyase activity step, Nucleic Acids Res. 29 (2001) 1285–1292.
[33] V.S. Sidorenko, G.A. Nevinsky, D.O. Zharkov, Mechanism of interaction between human 8-oxoguanine-DNA glycosylase and AP endonuclease, DNA Repair (Amst) 6 (2007) 317–328.
[34] H. Yang, W.M. Clendenin, D. Wong, B. Demple, M.M. Slupska, J.H. Chiang, J.H. Miller, Enhanced activity of adenine-DNA glycosylase (Myh) by apurinic/apyrimidinic endonuclease (Ape1) in mammalian base excision repair of an A/GO mismatch, Nucleic Acids Res. 29 (2001) 743–752.
[35] A. Parker, Y. Gu, W. Mahoney, S.H. Lee, K.K. Singh, A.L. Lu, Human homolog of the MutY repair protein (hMYH) physically interacts with proteins involved in long patch DNA base excision repair, J. Biol. Chem. 276 (2001) 5547–5555.
[36] P.J. Luncsford, B.A. Manvilla, D.N. Patterson, S.S. Malik, J. Jin, B.J. Hwang, R. Gunther, S. Kalvakolanu, L.J. Lipinski, W. Yuan, W. Lu, A.C. Drohat, A.L. Lu, E.A. Toth, Coordination of MYH DNA glycosylase and APE1 endonuclease activities via physical interactions, DNA Repair (Amst) 12 (2013) 1043–1052.
[37] M.A. Pope, S.L. Porello, S.S. David, Escherichia coli apurinic–apyrimidinic endonucleases enhance the turnover of the adenine glycosylase MutY with G:A substrates, J. Biol. Chem. 277 (2002) 22605–22615.
[38] D. Cortazar, C. Kunz, Y. Saito, R. Steinacher, P. Schar, The enigmatic thymine DNA glycosylase, DNA Repair (Amst) 6 (2007) 489–504.
[39] T.R. Waters, P. Gallinari, J. Jiricny, P.F. Swann, Human thymine DNA glycosylase binds to apurinic sites in DNA but is displaced by human apurinic endonuclease 1, J. Biol. Chem. 274 (1999) 67–74.
[40] C.V. Privezentzev, M. Saparbaev, J. Laval, The HAP1 protein stimulates the turnover of human mismatch-specific thymine-DNA-glycosylase to process 3, N(4)-ethenocytosine residues, Mutat. Res. 480–481 (2001) 277–284.
[41] U. Hardeland, R. Steinacher, J. Jiricny, P. Schar, Modification of the human thymine-DNA glycosylase by ubiquitin-like proteins facilitates enzymatic turnover, EMBO J. 21 (2002) 1456–1464.
[42] M.E. Fitzgerald, A.C. Drohat, Coordinating the initial steps of base excision repair. apurinic/apyrimidinic endonuclease 1 actively stimulates thymine DNA glycosylase by disrupting the product complex, J. Biol. Chem. 283 (2008) 32680–32690.
[43] M.R. Baldwin, P.J. O'Brien, Human AP endonuclease 1 stimulates multiple-turnover base excision by alkyladenine DNA glycosylase, Biochemistry 48 (2009) 6022–6033.
[44] M.R. Baldwin, P.J. O'Brien, Nonspecific DNA binding and coordination of the first two steps of base excision repair, Biochemistry 49 (2010) 7879–7891.
[45] R.L. Maher, A.C. Vallur, J.A. Feller, L.B. Bloom, Slow base excision by human alkyladenine DNA glycosylase limits the rate of formation of AP sites and AP endonuclease 1 does not stimulate base excision, DNA Repair (Amst) 6 (2007) 71–81.
[46] N.A. Kuznetsov, D.O. Zharkov, V.V. Koval, M. Buckle, O.S. Fedorova, Reversible chemical step and rate-limiting enzyme regeneration in the reaction catalyzed by formamidopyrimidine-DNA glycosylase, Biochemistry 48 (2009) 11335–11343.
[47] M. Saparbaev, S. Langouet, C.V. Privezentzev, F.P. Guengerich, H. Cai, R.H. Elder, J. Laval, 1, N(2)-ethenoguanine, a mutagenic DNA adduct, is a primary substrate of *Escherichia coli* mismatch-specific uracil-DNA glycosylase and human alkylpurine-DNA-N-glycosylase, J. Biol. Chem. 277 (2002) 26987–26993.
[48] N.A. Kuznetsov, V.V. Koval, D.O. Zharkov, G.A. Nevinsky, K.T. Douglas, O.S. Fedorova, Kinetics of substrate recognition and cleavage by human 8-oxoguanine-DNA glycosylase, Nucleic Acids Res. 33 (2005) 3919–3931.
[49] S. Daviet, S. Couve-Privat, L. Gros, K. Shinozuka, H. Ide, M. Saparbaev, A.A. Ishchenko, Major oxidative products of cytosine are substrates for the nucleotide incision repair pathway, DNA Repair (Amst) 6 (2007) 8–18.
[50] G. Golan, A.A. Ishchenko, B. Khassenov, G. Shoham, M.K. Saparbaev, Coupling of the nucleotide incision and 3′ → 5′ exonuclease activities in *Escherichia coli* endonuclease IV: structural and genetic evidences, Mutat. Res. 685 (2010) 70–79.
[51] S. Morera, I. Grin, A. Vigouroux, S. Couve, V. Henriot, M. Saparbaev, A.A. Ishchenko, Biochemical and structural characterization of the glycosylase domain of MBD4 bound to thymine and 5-hydroxymethyuracil-containing DNA, Nucleic Acids Res. 40 (2012) 9917–9926.
[52] N.A. Kuznetsov, V.V. Koval, G.A. Nevinsky, K.T. Douglas, D.O. Zharkov, O.S. Fedorova, Kinetic conformational analysis of human 8-oxoguanine-DNA glycosylase, J. Biol. Chem. 282 (2007) 1029–1038.
[53] N.A. Kuznetsov, V.V. Koval, D.O. Zharkov, Y.N. Vorobiev, G.A. Nevinsky, K.T. Douglas, O.S. Fedorova, Kinetic basis of lesion specificity and opposite-base specificity of *Escherichia coli* formamidopyrimidine-DNA glycosylase, Biochemistry 46 (2007) 424–435.
[54] V.V. Koval, N.A. Kuznetsov, A.A. Ishchenko, M.K. Saparbaev, O.S. Fedorova, Real-time studies of conformational dynamics of the repair enzyme *E. coli* formamidopyrimidine-DNA glycosylase and its DNA complexes during catalytic cycle, Mutat. Res. 685 (2010) 3–10.
[55] S.C. Brooks, S. Adhikary, E.H. Rubinson, B.F. Eichman, Recent advances in the structural mechanisms of DNA glycosylases, Biochim. Biophys. Acta 1834 (2013) 247–271.
[56] E.L. Rachofsky, R. Osman, J.B.A. Ross, Probing structure and dynamics of DNA with 2-aminopurine: effects of local environment on fluorescence, Biochemistry 40 (2001) 946–956.
[57] J.M. Jean, K.B. Hall, 2-Aminopurine fluorescence quenching and lifetimes: role of base stacking, Proc. Natl. Acad. Sci. U. S. A. 98 (2001) 37–41.
[58] L.Y. Kanazhevskaya, V.V. Koval, Y.N. Vorobjev, O.S. Fedorova, Conformational dynamics of abasic DNA upon interactions with AP endonuclease 1 revealed by stopped-flow fluorescence analysis, Biochemistry 51 (2012) 1306–1321.
[59] P.C. Blainey, A.M. van Oijen, A. Banerjee, G.L. Verdine, X.S. Xie, A base-excision DNA-repair protein finds intrahelical lesion bases by fast sliding in contact with DNA, Proc. Natl. Acad. Sci. U. S. A. 103 (2006) 5752–5757.
[60] A.A. Kuznetsova, N.A. Kuznetsov, A.A. Ishchenko, M.K. Saparbaev, O.S. Fedorova, Step-by-step mechanism of DNA damage recognition by human 8-oxoguanine DNA glycosylase, Biochim. Biophys. Acta 1840 (2014) 387–395.
[61] N.A. Kuznetsov, A.A. Kuznetsova, Y.N. Vorobjev, L.N. Krasnoperov, O.S. Fedorova, Thermodynamics of the DNA damage repair steps of human 8-oxoguanine DNA glycosylase, PLoS One 9 (2014) e98495.
[62] S.D. Bruner, D.P. Norman, G.L. Verdine, Structural basis for recognition and repair of the endogenous mutagen 8-oxoguanine in DNA, Nature 403 (2000) 859–866.
[63] S. Doublie, V. Bandaru, J.P. Bond, S.S. Wallace, The crystal structure of human endonuclease VIII-like 1 (NEIL1) reveals a zincless finger motif required for glycosylase activity, Proc. Natl. Acad. Sci. U. S. A. 101 (2004) 10284–10289.
[64] A.Y. Lau, O.D. Scharer, L. Samson, G.L. Verdine, T. Ellenberger, Crystal structure of a human alkylbase-DNA repair enzyme complexed to DNA: mechanisms for nucleotide flipping and base excision, Cell 95 (1998) 249–258.
[65] A.Y. Lau, M.D. Wyatt, B.J. Glassner, L.D. Samson, T. Ellenberger, Molecular basis for discriminating between normal and damaged bases by the human alkyladenine glycosylase, AAG, Proc. Natl. Acad. Sci. U. S. A. 97 (2000) 13573–13578.
[66] D.P. Norman, S.D. Bruner, G.L. Verdine, Coupling of substrate recognition and catalysis by a human base-excision DNA repair protein, J. Am. Chem. Soc. 123 (2001) 359–360.
[67] B.A. Manvilla, A. Maiti, M.C. Begley, E.A. Toth, A.C. Drohat, Crystal structure of human methyl-binding domain IV glycosylase bound to abasic DNA, J. Mol. Biol. 420 (2012) 164–175.
[68] H. Hashimoto, X. Zhang, X. Cheng, Excision of thymine and 5-hydroxymethyluracil by the MBD4 DNA glycosylase domain: structural basis and implications for active DNA demethylation, Nucleic Acids Res. 40 (2012) 8276–8284.
[69] C.D. Mol, T. Izumi, S. Mitra, J.A. Tainer, DNA-bound structures and mutants reveal abasic DNA binding by APE1 and DNA repair coordination, Nature 403 (2000) 451–456.
[70] S.E. Tsutakawa, D.S. Shin, C.D. Mol, T. Izumi, A.S. Arvai, A.K. Mantha, B. Szczesny, I.N. Ivanov, D.J. Hosfield, B. Maiti, M.E. Pique, K.A. Frankel, K. Hitomi, R.P. Cunningham, S. Mitra, J.A. Tainer, Conserved structural chemistry for incision activity in structurally non-homologous apurinic/apyrimidinic endonuclease APE1 and endonuclease IV DNA repair enzymes, J. Biol. Chem. 288 (2013) 8445–8455.
[71] J.D. Schonhoft, J.T. Stivers, Timing facilitated site transfer of an enzyme on DNA, Nat. Chem. Biol. 8 (2012) 205–210.